GOODYEAR AEROSPACE
CORPORATION
AKRON 15, OHIO

STUDY OF EXPANDABLE, TERMINAL DECELERATORS FOR MARS ATMOSPHERE ENTRY, INTERIM SUMMARY REPORT

GER-12691, Rev A 22 July 1966

This work was performed for the Jet Propulsion Laboratory, California Institute of Technology, sponsored by the National Aeronautics and Space Administration under Contract NAS7-100.

Prepared by

Jay L. Musil

FOREWORD

The work presented in this report was performed by Goodyear Aerospace Corporation, subsidiary of The Goodyear Tire and Rubber Company, Akron, Ohio, for the Jet Propulsion Laboratory, California Institute of Technology, under the authority of Contract No. 951153. The period covered is from December 1965 to June 1966. Mr. James M. Brayshaw, Jr., is the Jet Propulsion Laboratory Technical Representative.

The effort is being performed under the general direction of Mr. R. L. Ravenscraft, manager of the Aero-Mechanical Engineering Division and Mr. Fred R. Nebiker, manager of the Recovery Systems Engineering Department. The program is being directed by Mr. Jay L. Musil, serving as project engineer.

TABLE OF CONTENTS

LIST OF ILLUSTRATIONS

SECTION I - DESCRIPTION OF PROGRAM

1. INTRODUCTION

Goodyear Aerospace Corporation (GAC) is conducting a parametric study to determine the suitability of expandable terminal decelerators for a Mars-lander capsule. Under the terms of Contract No. 951153 from the Jet Propulsion Laboratory (JPL), the study is based on the analytical formulation of the effects associated with the model environments of Mars and specified capsule entry conditions. These effects and conditions govern the requirements for the engineering applications of expandable decelerator devices.

The main objective (see Figure 1) is to determine fundamental engineering system design requirements for initial-stage, expandable decelerators

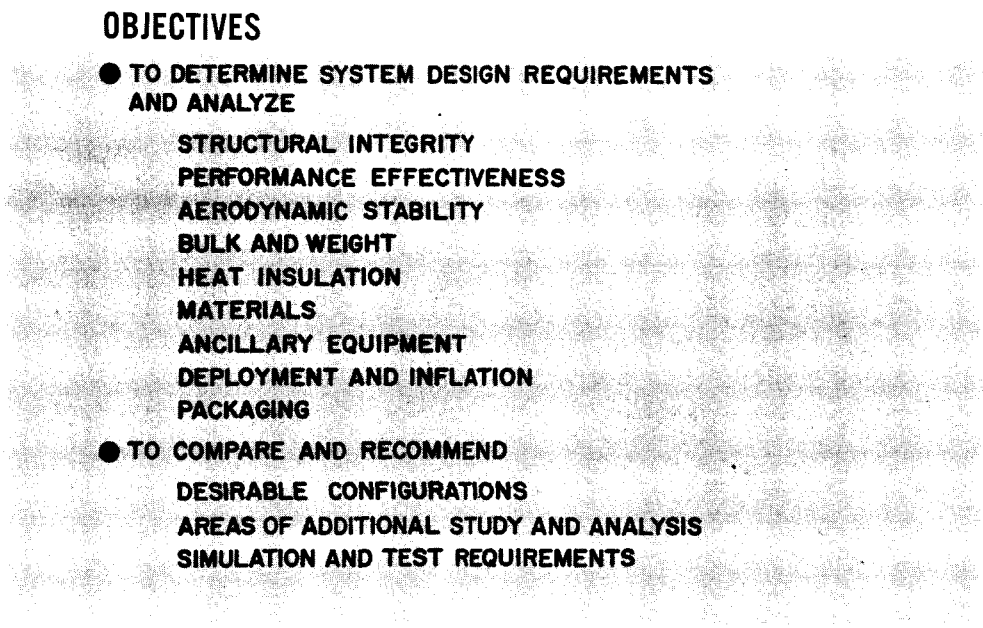

Figure 1

that must stabilize and retard the Mars-lander capsule. The characteristics of various expandable decelerators are being determined by the formulation of uncomplicated engineering techniques of analysis and design. Then, desirable configurations that will retard capsules to about Mach number 1 at 10,000, 20,000, and 30,000 ft above the Martian terrain will be selected and recommended.

Figure 2 illustrates the interrelationships of aerodynamic decelerator applications to the Voyager lander program; the requirements and technology breakdowns for the Voyager program are related directly to those in the present program.

2. EXISTING ANALYSIS PROCEDURE

To date, aerodynamic decelerator system design has depended primarily on the available technology developed from specialized previous applications and investigations. The accepted method for establishing a design for a new application has included the procedure indicated by Figure 3:

1. Survey of performance data relating to various decelerator configurations
2. Evaluation of these data to determine the extent that a particular configuration and operating conditions relate to the specified requirements for the new application
3. Conducting a preliminary design effort and building test models
4. Conducting wind-tunnel, functional, and environmental tests to establish validity of the predicted performance of a specific design for the new application and operating environments
5. Designing, building, and conducting full-scale, free-flight tests of the decelerator system under simulated operational conditions and environments

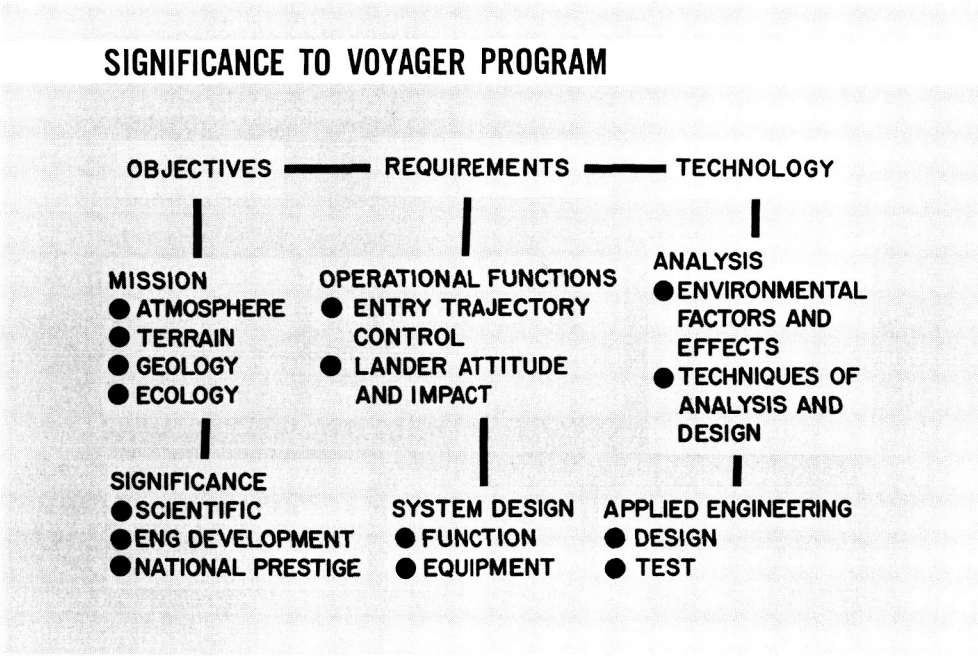

Figure 2

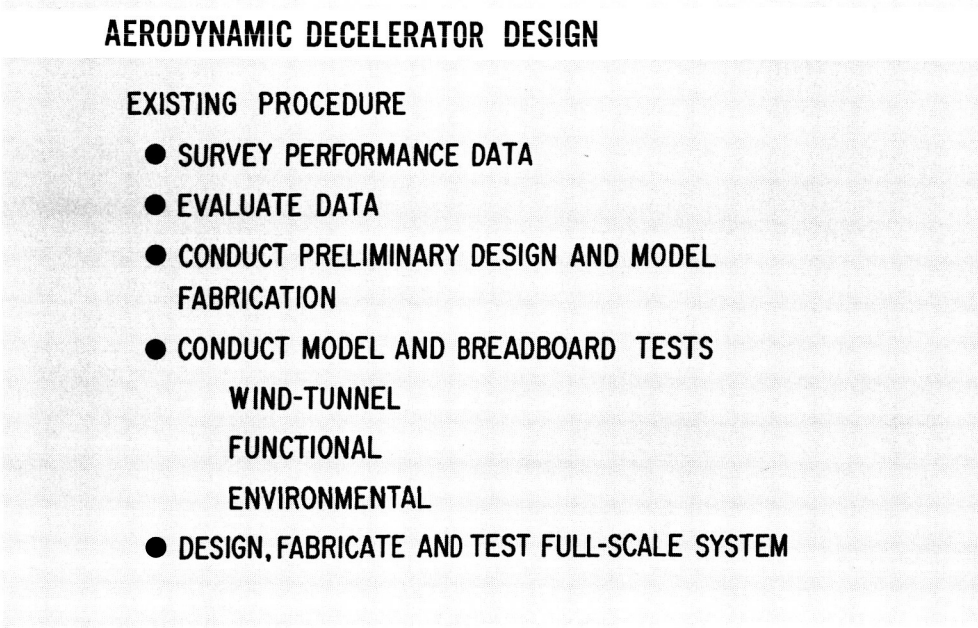

Figure 3

These procedures and their sequence have been demonstrated successfully. However, they have been carried out too often with the expense of unscheduled, additional time and cost for redesign and retest. One of the major difficulties encountered was the extrapolation of system design data from previous applications. In many cases and usually after the program was well underway, the available data were found to be inadequate or not applicable and as a result, iteration of Steps 3, 4, and 5 was required. Additionally, procedures and time scales establishing requirements for aerodynamic decelerator applications were often incompatible with the development of the most reliable and efficient decelerator system design.

3. PRESENT ANALYSIS APPROACH

The present program, comprising a parameter study, has taken a different approach to evaluating the characteristics of aerodynamic decelerator devices as compared with the analysis procedure outlined by Figure 3. To illustrate the present approach, Figure 4 shows a functional flow diagram of the factors and variable parameters appropriate to the application of aerodynamic decelerator devices for trajectory control of planetary entry vehicles. The inputs and outputs are associated with the environments, constraints, requirements, and objectives of the present study. The simplicity of the functional diagram is somewhat deceptive. If a servo circuit is used as an analogy, the system is "open-loop," which at once points up the inherent difficulty of aerodynamic decelerator design technology. "Matching" (i.e., achieving an optimized design) of the parameters and factors for a desirable system must be accomplished by techniques similar to the graphic solutions for some types of mathematical equations involving transcendental functions.

In reality there is, of course, feedback through the dynamic characteristics of the physical system as a result of coupling through the external operating environment and the resulting system motions. Unfortunately,

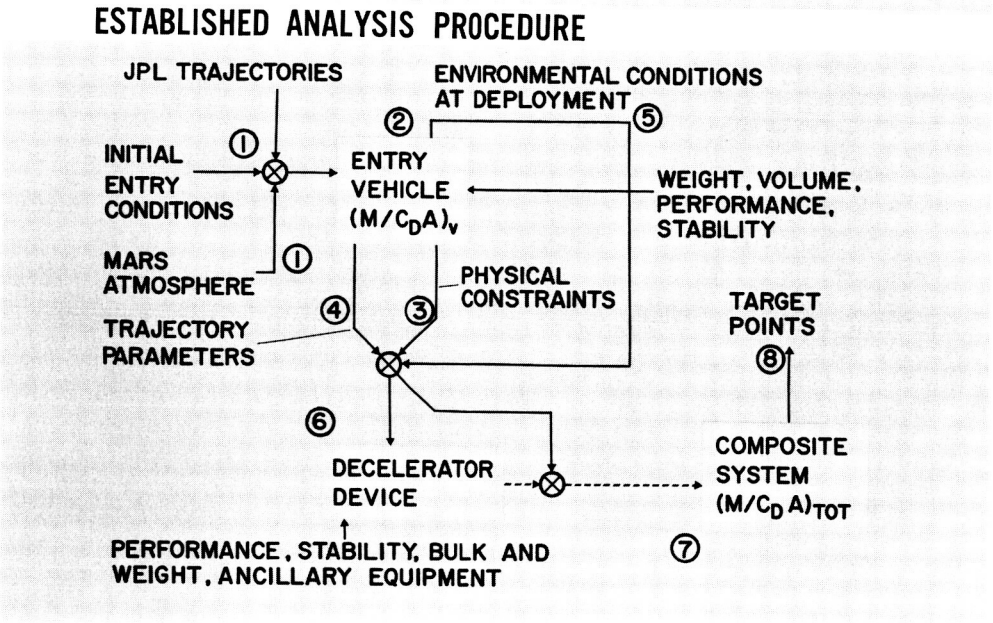

Figure 4

this feedback is quite nonlinear by the very nature of the performance characteristics of aerodynamic decelerator devices when moving through an atmosphere at high speeds, necessitating adaptation of the parameters to the desired system performance.

The purpose of this discussion is not to emphasize the difficulty of the present study, but rather to demonstrate the validity of the uncomplicated, but nevertheless straightforward engineering analysis approach and procedures established for this program. Furthermore, this analysis is considered appropriate since it permits evaluation for all possible aerodynamic decelerator system concepts.

As shown by Figure 4, the significant factors and parameters that must be considered and evaluated in establishing the design of a deployable aerodynamic decelerator system for the Mars-lander capsule include:

1. Initial entry conditions (V_e, γ_e) associated with the designated JPL trajectories (A1, A4, B1, B3

19, 22, 23, 30, 37) and the characteristics of the Mars atmosphere (VM3, VM4, VM7, VM8)

2. Basic entry-vehicle characteristics
3. Physical constraints on the decelerator device bulk, weight, configuration, attachments, etc.
4. Resulting trajectory parameters (M, h, γ, θ, etc.) that indicate the permissible time-distance scales for the decelerator device operation
5. Environmental conditions at deployment (T_o, q, g's, θ, etc.) and operation of the decelerator that establish design requirements for the device performance and structural integrity
6. Decelerator device characteristics as related to performance, stability, weight, and bulk
7. Composite system characteristics
8. Target points of Mach number, altitude, angular excursions, and attitude rates

The interrelated factors and parameters affecting the application of aerodynamic decelerator devices are complex and no direct or precise solution is possible. Analysis of the factors and effects must be studied in discrete, uncomplicated, and orderly fashion and then the separate results for a composite system as applied to representative operational cases must be synthesized. After definitive trends have been established, indicating the more-favorable configurations, selections are made. Refined analyses and investigations are performed leading to the final selection of the system worthy of full-scale development and application.

SECTION II - REVIEW OF RESULTS FROM ANALYSES

1. CONSIDERATION OF BASIC DECELERATOR CONFIGURATIONS

For the present study, a basic entry capsule has been specified having a blunted cone configuration, as shown in Figure 5. The capsule has an included angle of 120 deg and the characteristics indicated in the table in Figure 5.

The study has allowed substantial volume availability and a minimum of interface constraints so that assessment of the various decelerator configurations are not restricted by this consideration.

An inflatable AIRMAT[a] cone, which is an extension of the basic entry body angle, and ram-air, self-inflating BALLUTE[a] devices schematically illustrated in Figure 6 have been considered in the present program. The characteristic trends for these configurations resulting from the analyses performed will be shown in subsequent figures. They are indicative of all expandable, pressure-inflatable devices, including parachutes and other balloon-like configurations that require auxiliary gas inflation sources. Only the values indicated for the represented cases and configurations will change.

The analytical tools that have been employed to generate the results to date have included point-mass trajectory computations, generalized strength/weight analyses, drag performance estimates, pressure distribution estimates, materials investigations, and thermal analyses (see Appendix A).

Some discussion relating to the trailing and attached plain-back BALLUTE configuration is appropriate at this point. These configurations are shown

[a]TM, Goodyear Aerospace Corporation, Akron, Ohio. 44315

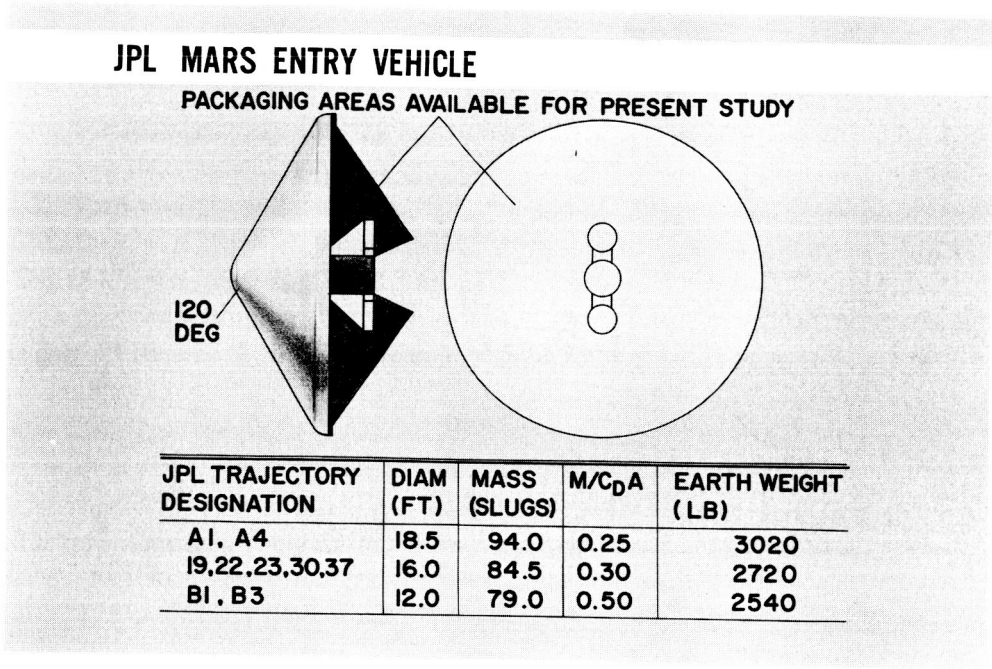

JPL TRAJECTORY DESIGNATION	DIAM (FT)	MASS (SLUGS)	M/C_DA	EARTH WEIGHT (LB)
A1, A4	18.5	94.0	0.25	3020
19,22,23,30,37	16.0	84.5	0.30	2720
B1, B3	12.0	79.0	0.50	2540

Figure 5

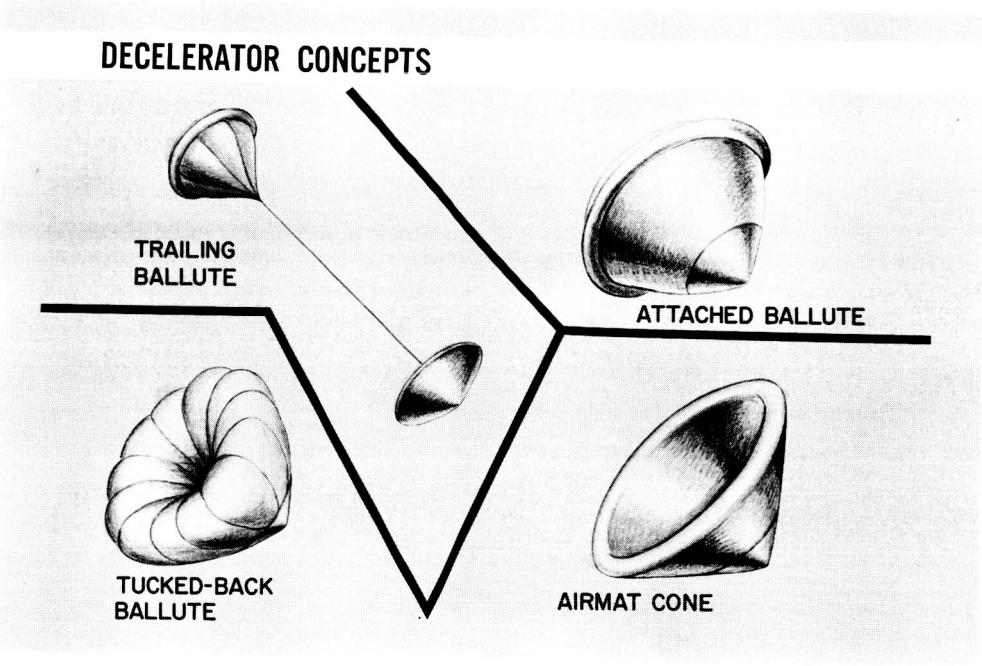

Figure 6

with burble fences positioned circumferentially approximately 15 deg aft of the maximum BALLUTE diameter. There are various aerodynamic and structural considerations for the use of the fence, one of which is to establish a point of uniform viscous separation near the maximum diameter of the BALLUTE. Although this consideration is associated primarily with subsonic speeds, i.e., before the critical (local sonic) Mach number is encountered at the maximum BALLUTE diameter, there is a possibility of encountering a similar effect for a range of transonic Mach numbers above 1.0. The phenomena of the nonuniform separation associated with BALLUTE-like devices without the fence is the same as the oscillating of a child's balloon when trailed from a moving automobile.

Additionally, the fence projection provides a substantial portion of the overall drag of the BALLUTE and can produce the same drag as a much larger BALLUTE without a fence. Strength, bulk, and weight requirements can be correspondingly less for a given drag effectiveness requirement. It has been found from tests that fence projections as high as 20 percent of the BALLUTE radius are effective. This amount of fence projection provides a 44 percent increase in relation to the BALLUTE reference area and at the same time, the desired uniform viscous separation effect is ensured. It is possible that a fence of a form similar to that described may be a desirable incorporation for the tucked-back BALLUTE.

The effect of the riser line on the decelerator system weight is an important consideration with respect to the trailing BALLUTE configuration (incidentally, this consideration also is true for trailing parachute decelerators). GAC's analyses indicate that for a BALLUTE that trails at a distance of four capsule base diameters in the operational environment of interest, the weight breakdown will be approximately 20 percent for the BALLUTE envelope, 33 percent for the meridian cables, 15 percent for coating (considering both heat insulation and porosity), and 32 percent for the riser. As will be shown subsequently, the high percentage of weight attributable to the riser results in the disappointing fact that trailing

decelerator devices can have less-favorable weight fractions than attached BALLUTE configurations, even though the physical size of the trailing decelerator is smaller.

2. ATMOSPHERE AND TRAJECTORY CONSIDERATIONS

Figure 7 shows the Mars entry trajectories in the VM7 and VM8 atmosphere profiles for the basic entry vehicle configuration previously illustrated in Figure 5. Seven entry trajectories have been selected by JPL for the basic entry capsule to establish the environmental conditions under which the decelerators must perform successfully with structural integrity. The initial entry velocities and angles, and mass ballistic coefficients associated with the corresponding trajectories are given in Table I. Two additional trajectories (one each in the VM3 and VM4 atmospheres) will be investigated to determine effects of atmosphere variation for off-design conditions, influenced mainly by the thermal heat pulse.

Due consideration also is being given to such controlling factors as entry

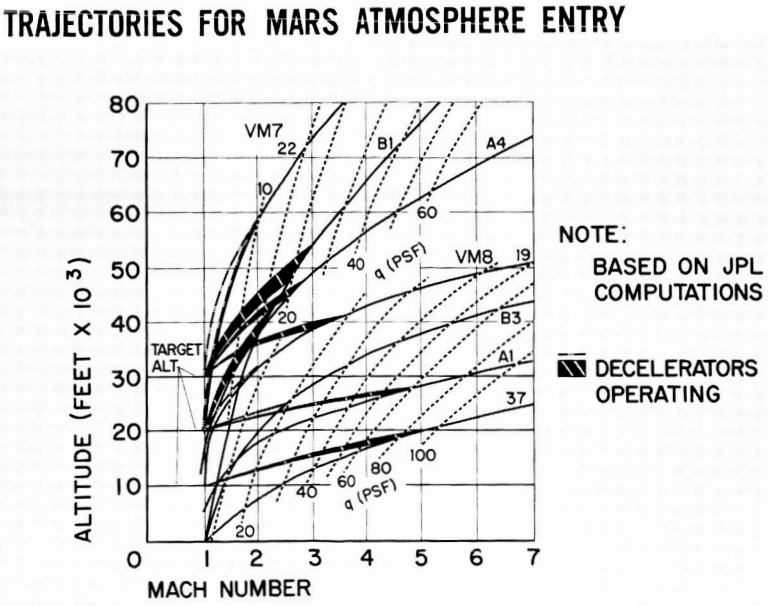

Figure 7

TABLE I - INITIAL ENTRY CONDITIONS

JPL trajectory designation	Entry velocity, V_e (fps)	Entry angle, γ_e (deg)	Capsule mass ballistic parameter, $M/C_D A$ (slugs/sq ft)	Atmosphere profile
A1	23,000	25	0.25	VM8
A4	23,000	25	0.25	VM7
B1	15,000	15	0.5	VM7
B3	15,000	15	0.5	VM8
19	16,000	16	0.3	VM8
22	16,000	16	0.3	VM7
37	23,000	28	0.3	VM8

vehicle size and configuration, sterilization requirements, and the entry trajectories and Mach number/altitude targets mentioned previously.

Although the surface density for the projected Mars VM8 atmosphere (ρ_o = 2.56×10^{-5} slugs/cu ft) is almost twice that of the VM7, the inverse scale height above the tropopause is greater by a factor of about 2.8. Thus, for a capsule with a given mass-ballistic coefficient and having the same initial entry conditions, there are shorter time scales, lower altitudes, and higher dynamic pressures associated with deceleration of the basic entry capsule to the same target Mach number/altitudes in the VM8 atmosphere as compared with the VM7. Consequently, entry in the VM8 atmosphere will establish the criteria for the design integrity of an initial-stage supersonic decelerator, since higher Mach number performance is required and correspondingly higher aerodynamic pressure loads are encountered.

It should be brought out that higher driving temperatures are associated with the VM7 atmosphere at corresponding Mach numbers. However, in this atmosphere the results of analyses indicate a trend toward considerably lower deployment Mach number requirements ($M \leq 3.0$ for h_t = 30,000 ft or 20,000 ft) for first-stage decelerators. This trend minimizes

aerodynamic heating effects as a critical design factor for the cases being considered in this study.

The remaining discussion will be with specific reference to the A1, A4, and 19-configuration trajectories. However, the analysis procedures and characteristic trends indicated are appropriate to all the cases. Note that the A1 and A4 trajectories are associated with a higher initial entry velocity and steeper entry angle (V_e = 23,000 fps; γ_e = 25 deg) as compared to the other entry cases with the exception of the 37-configuration trajectory. One may consider that these entry conditions are associated with lower accuracy constraints for either the orbiting or the fly-by entry modes for the capsule. As shown by the trajectories of Figure 7, it is indicated that the severity of environmental conditions encountered at corresponding altitudes in the VM8 atmosphere are affected more substantially by initial entry conditions than by the mass-ballistic parameter. Consequently, it should be recognized that the results (discussed later pertaining to the A1 configuration trajectory) indicate less favorable weight fractions for first-stage decelerators to achieve the same target Mach number/altitude points as compared with the 19-configuration trajectory. The 19 trajectory has a lower initial entry V_e (16,000 fps) and a lower γ_e (16 deg) with a higher mass-ballistic parameter M/C_DA of 0.3.

3. INITIAL STAGE DECELERATOR CONFIGURATIONS

Figure 8 shows the drag coefficient variation with Mach number for the configurations illustrated in Figure 6. For the attached and trailing BALLUTES and the conical flare configurations, there are various sources of data for reasonable engineering confidence in the drag variations indicated throughout the Mach number range of current interest. There are no comparable data for the tucked-back BALLUTE. However, for purposes of this study, a reasonable approximation is possible for the drag coefficient based on the characteristic trends for blunt, large-angle cone configurations.

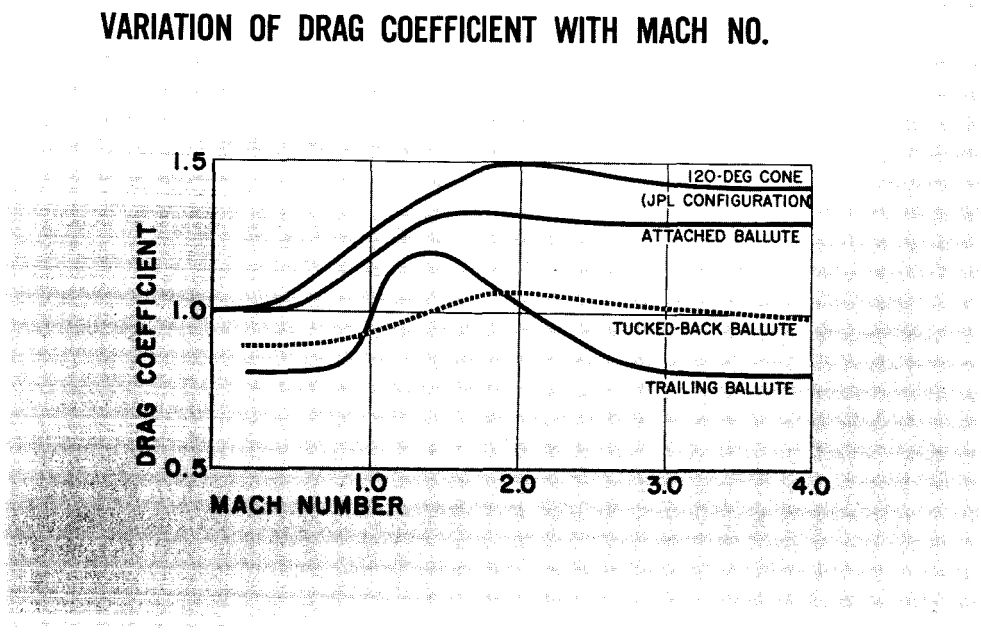

Figure 8

The drag coefficient variation for the trailing BALLUTE shown in Figure 8 is associated with BALLUTE-to-forebody diameter ratios in the range from 1.0 to about 3.0. The characteristic reduction in drag effectiveness with increasing Mach numbers primarily is caused by the reduction of energy in the forebody wake and the wake flow conditions. Numerous tests have demonstrated the good drag effectiveness and low-oscillation characteristics of the BALLUTE trailing at a distance within less than four forebody base diameters. The BALLUTE-to-forebody diameter ratios were in the range from 1.0 to 3.0 over a Mach number range from 0.1 to 10.0. Other trailing decelerator configurations for supersonic applications, including variations of the Hyperflo parachute family, generally have to be positioned farther aft of the forebody base. They also require a larger diameter to develop the equivalent drag effectiveness of the BALLUTE configuration incorporating a 10 percent burble fence. Furthermore, the characteristic blunt face of the parachute canopy gives rise to exaggerated unsteady flow conditions at supersonic speeds, generally causing violent

parachute flutter and instability at off-design Mach numbers. This phenomenon is not associated with ram-air inflated BALLUTE devices during operation primarily because of the more steady and uniform flow directed over the symmetrical forward portion and the strong damping and rigidizing effect of the entrapped stagnation (i.e., total) pressure within the inflated BALLUTE envelope.

4. EVALUATION OF RESULTS

Figure 9 indicates the decelerator device size requirements to accomplish deceleration of the A1, A4, and 19 entry configurations to a target Mach number of 1.0 at target altitudes of 20,000 and 30,000 ft above the terrain. The decelerators are assumed to be developing their full drag effectiveness at the corresponding Mach numbers on the abscissa scale. In other words, time scales for decelerator device deployment and inflation are not reflected in these results. It must be noted, therefore, that for the corresponding Mach numbers in Figures 9, 10, and 12, there is

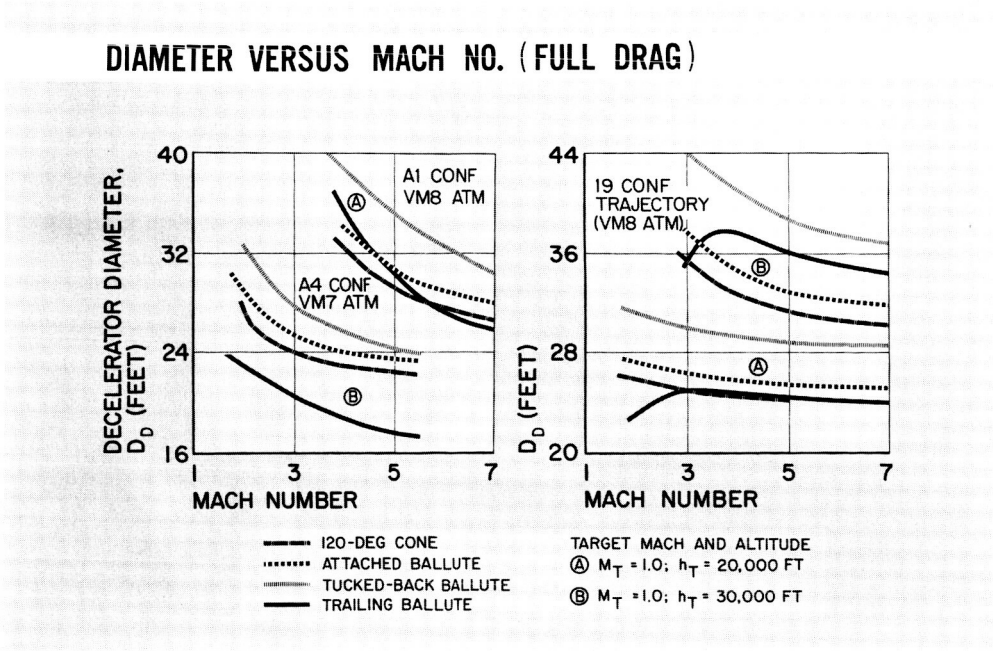

Figure 9

a slightly higher Mach number (approximately 5 percent) and dynamic pressure at which the decelerator device is deployed initially and begins to inflate. Figure 9 shows the interesting trend to asymptotic values of decelerator size as Mach number is increased. Thus, in relation to the size of a decelerator, an upper limit to the Mach numbers is indicated above which there is no appreciable gain (i.e., reduction in decelerator size) in employing a decelerator to achieve lower specific target Mach number/altitude points. In comparing the curves associated with the target point Mach number of 1.0 and the 20,000-ft altitude for the trajectory of configuration 19, the expected smaller decelerator sizes are indicated as a result of the increasing density of the atmosphere.

Figure 10 presents the percent of decelerator weight to total system weight for the four decelerator configurations considered and as applied to the A1, A4, and 19 configuration entry trajectories.

The decelerator strength requirements are predicated on the use of Dacron

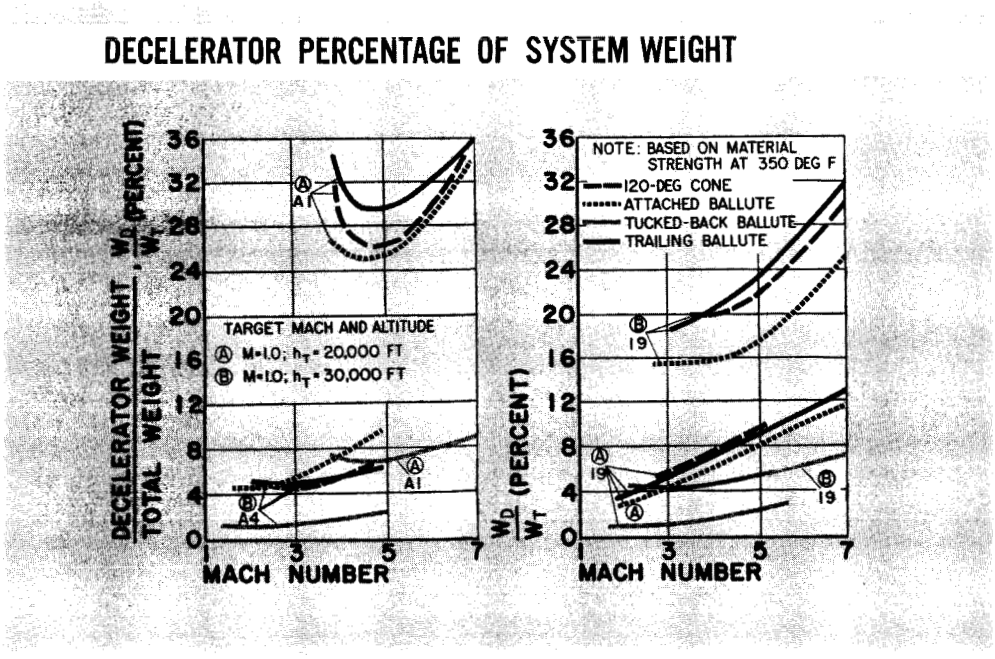

Figure 10

material operating at an elevated temperature of 350 F. A material strength design factor of 2.0 is also reflected in the results presented.

When it is possible to attain specified target altitude/Mach number conditions within physical constraints and within allowable time and distance scales, Figures 9 and 10 indicate that it is desirable to accept a larger decelerator diameter and delay operation of the device to a corresponding lower Mach number. This consideration leads to the interesting trend of arriving at a minimum percentage of decelerator weight and corresponding optimum initial operating Mach number. For the trajectory of configuration 19 and the case of the target points of M = 1 and 20,000-ft altitude, the same trends are indicated. However, as a result of the extended available time and distance scales and higher atmosphere density, the values for the decelerator size, weight fraction, and operational Mach number are all substantially reduced. The interaction of Mach number effect (i.e., dynamic pressure) on the decelerator strength and weight requirements has a compounding effect.

The weight for a flexible, pressure-inflated decelerator as shown by Figure 11 is related to:

$$w_D = f(P, D^3, K_1, K_2)$$

where P is pressure; D, diameter; K_1, a shape factor; and K_2, a material strength factor. The pressure P for a ram-air inflatable BALLUTE device is a function of the configuration, dynamic pressure, and the flow conditions of the operating environment. For design purposes and structural integrity, maximum values of the parameters corresponding to the deployment conditions are employed in any particular design application. The primary criterion is the pressure recovery at the ram-air inlets of the device. Numerous tests and analyses have shown that by making judicious consideration of geometry and position effects, an almost constant pressure recovery factor of 2.75 at the inlets can be achieved for deployment Mach numbers above about 2.0.

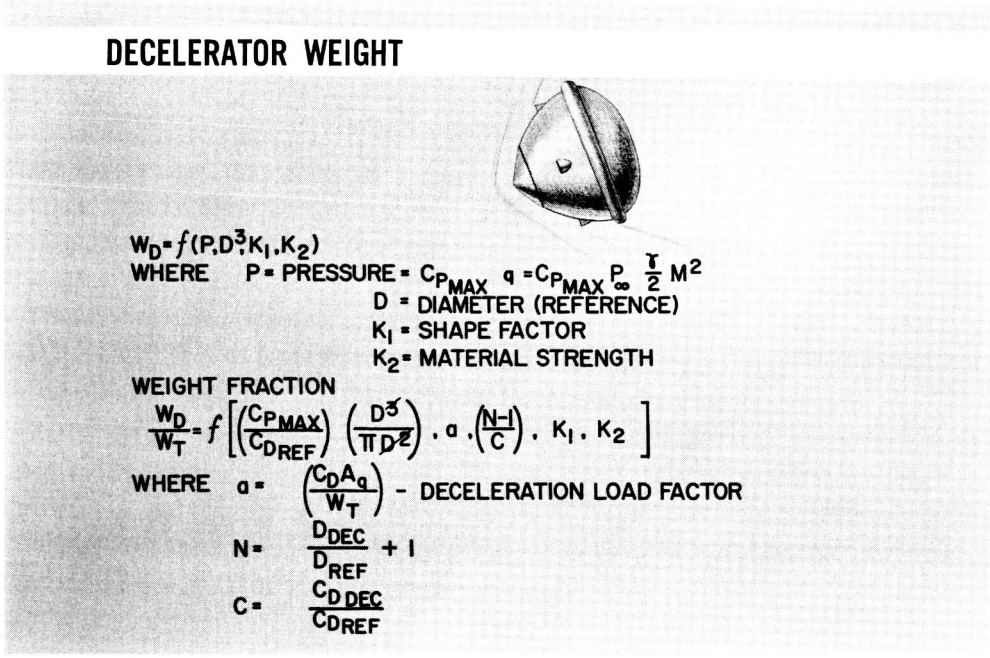

Figure 11

In terms of a weight ratio, it can be shown that the decelerator weight fraction increases directly with diameter. This fact reflects the disappointing but well known effect of the cube square law for structural scaling with increasing size. Additionally, the decelerator weight fraction is also a function of the dynamic pressure or square of the Mach number. Therefore, it is related to the external surface pressure that requires support by the pressure within the device.

Thus, the results presented by Figure 10 and the interpretations obtained and described were developed from static aerodynamic loading relationships with empirically determined, quasi-static load, temperature, and design factors employed to account for operating environmental effects and material characteristics. This approach has been demonstrated to be safe and reliable, although at times resulting in conservative or somewhat less than optimum designs. Considering dynamic loading effects, however, additional weight advantages may be gained by delaying the

decelerator device deployment to lower dynamic pressure conditions, when time and distance scales permit, for the following reasons:

1. Energy requirements to deploy and erect a decelerator device are reduced since the vehicle system is inertially decelerating at a lower rate
2. Snatch loads on the decelerator device, supporting structure, and vehicle as a result of lower relative inertial velocities are reduced
3. Deployment opening shock and inflation loads are reduced as a result of lower dynamic pressures
4. Peak heat flux, integrated heat load, and maximum temperature rise on exposed surfaces of the decelerator are reduced as a result of the lower deployment velocity and shorter time scales of operation to attain lower specified target altitude/Mach number conditions

Figure 12 has been developed to indicate the degree of validity in choosing Dacron material when operating at a temperature of 350 F for the decelerator devices analyzed and in leading to the results presented in Figures 9 and 10 for the A1 and 19 trajectories. The thermal requirement curves for Dacron and Nomex for the A1 configuration represent the fabric weight per unit area required to limit the total temperature rise to 350 F in the case of Dacron and 600 F in the case of Nomex. These curves correspond with the decelerator sizes in Figure 9 that begin effective operation att the corresponding Mach number on the abscissa scale. The material temperature results from the heat flux and integrated heat load corresponding with the velocity-time-distance scales (appropriate to initial operating conditions for the decelerators) to achieve the target points of M = 1.0 and 20,000-ft altitude. Boundaries for both 30,000- and 20,000-ft target altitudes for the 19 configuration have been included in Figure 12 to

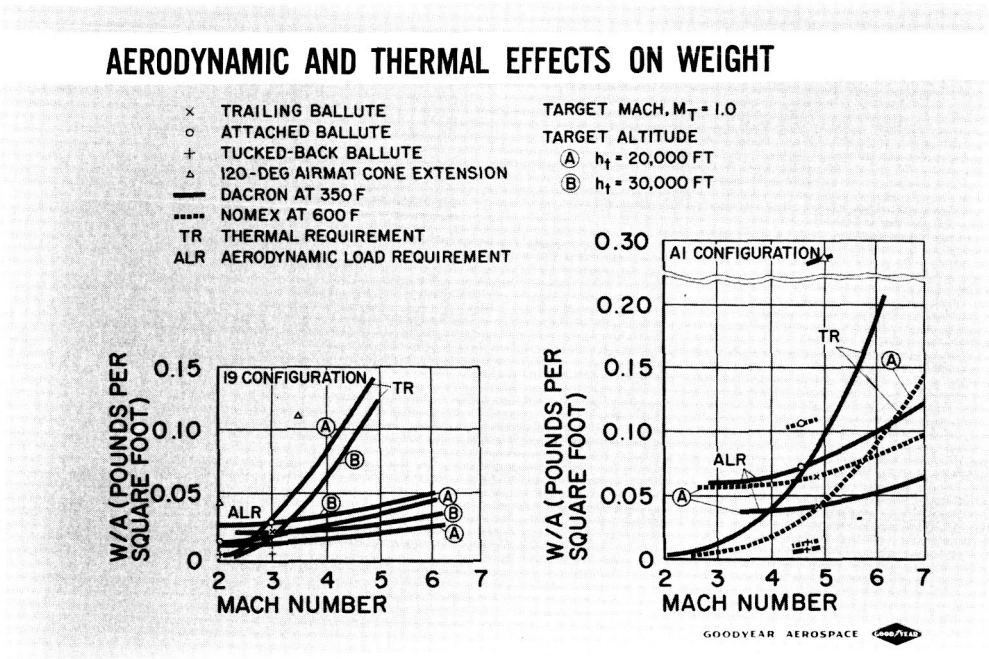

Figure 12

indicate the effect of a lower target altitude requirement. For the lower target altitude, there are associated lower initial operating Mach number requirements with the resulting fact that aerodynamic heating effects are minimized. To develop the thermal requirement curves, the heat absorbed by the decelerator material was simply assumed to be that of its heat capacity.

Superimposed on Figure 12 are the curves of decelerator device fabric weight per unit area as determined by the aerodynamic loading requirements for the target point conditions. For the A1 configuration with target conditions of M_T = 1.0 and h_T = 20,000 ft, it is shown that the assumption of Dacron material to be used at a 350-F "static" temperature for the 120-deg conical AIRMAT flare configuration (initially operating at the indicated optimum Mach number from Figure 10) is conservative. For the attached BALLUTE, the assumption is quite accurate; for the trailing and tucked-back BALLUTEs, the assumption is optimistic.

It is pointed out that the static strength/weight analysis and the thermal

analysis did not include provision for coating weight. Some coating must be provided in any event to ensure minimum acceptable leakage rates to maintain the desired pressurization within the decelerator envelope. Typical coating materials employed for this purpose are also good heat insulating materials. Nominal thicknesses of coatings of the order of 0.01 psf of the Vitron or Neoprene type will provide a net porosity of about 0.02 cu ft/sq ft/sec, generally considered as an acceptable value from experience for the upper values of pressure ratios and operating environments encountered for this study.

The fabric weight per unit area is in reference to the thin envelope of the decelerator device. The proportion of envelope weight to total decelerator weight is nominally 20 percent for the trailing BALLUTE, 38 percent for the attached BALLUTE, and 10 percent for the tucked-back BALLUTE. For the 120-deg AIRMAT cone, the envelope comprises about two-thirds of the total weight. Furthermore, for the cases under study, the period of the significant heat pulse is of the order of 10 sec. In this interval the capsule/decelerator combination will have reduced its speed significantly and the corresponding aerodynamic loads will be much smaller by the time the material reaches the assumed operating temperature of 350 F as used in the present study. Thus, it is indicated that for coating unit weight requirements, based on acceptable leakage rate and heat insulation, there would not be substantial increases in the overall decelerator weight fractions above that shown by Figure 10.

The determination of how the decelerator size and target altitude were affected by the target point Mach number as it varied from 0.7 to 1.5 is important also. Figure 13 illustrates these effects for the 19-configuration trajectory. Considering the effect on size, increasing target Mach number to 1.4 results in a reduction of total system drag area by the increment of about 100 percent from the value required at Mach 1.0. In this case, this corresponds to decreasing the decelerator diameter by about 10 percent for an initial operating Mach number of 3.0. The trend

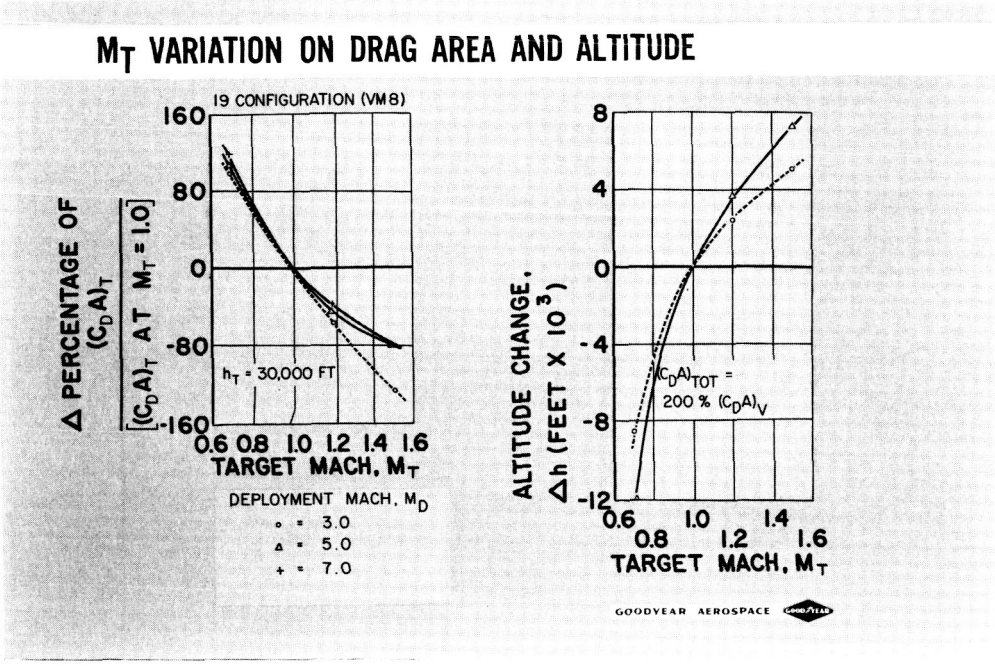

Figure 13

is for a lesser reduction in size with higher initial operating Mach number. On the other hand, for a lower target Mach number of 0.7, a 10 percent increase in decelerator size is indicated assuming a constant value of drag coefficient that is optimistic. At the subsonic target Mach numbers, the effect of the initial operating Mach number is nominal. The same type of trend is exhibited in the case of altitude variation at a constant value of decelerator drag area. In other words, if the target Mach number is allowed to increase above 1.0 there is an incremental gain in target altitude. The effect is the converse for decreasing values of target point Mach number. Again, in the case of higher target Mach numbers, the effect of the higher initial operating Mach number results in an additional gain in altitude primarily because the higher Mach number is also associated with a higher initial operating altitude. On the other hand for lower target Mach numbers, the effect of a higher initial operating Mach number results in a further loss in altitude. This occurs because the required decelerator drag area corresponding with the

higher initial operating Mach number is smaller to achieve the reference target Mach number of 1.0.

SECTION III - ADDITIONAL INVESTIGATIONS

The comparison and selection of decelerator configurations and their points of application for final study and analysis (see Figure 14) have been facilitated by a tabulation scheme (see Appendix B). Twenty-nine separate factors associated with the characteristics of each of the four decelerator configurations under study are evaluated. The tabulation includes those factors that establish realistic total decelerator system weight estimates and that are necessary for use with the dynamic computer analyses.

In addition to the comparison and selection effort, Figure 14 shows that refined point-mass trajectories incorporating a transient, heat-transfer analysis program are being conducted with the selected configurations. The computations include provision for a linear increase in decelerator drag area from

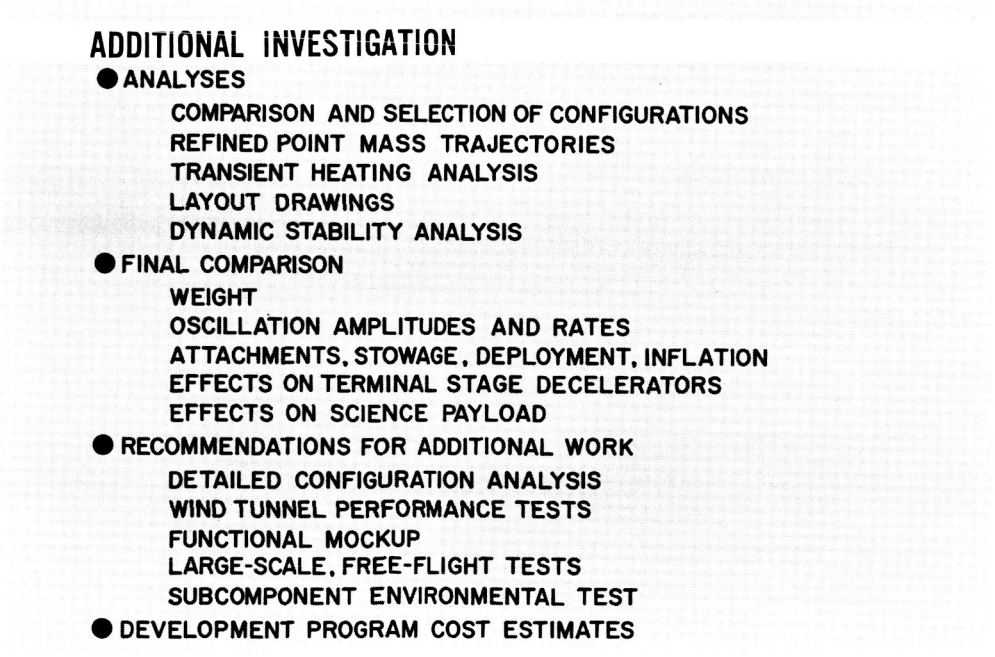

Figure 14

initiation of deployment to full inflation in an interval of 1.5 sec. The assumption of this inflation interval and linear drag area variation is based on experience with ram-air-inflated BALLUTE devices for the Mach number and dynamic pressure range of current interest. It includes tradeoff considerations of a minimum desired time to full-drag effectiveness, low opening shock, and material fatigue failure as a result of flutter during the inflation interval. Of course, it was necessary in the case of the ram-air-inflated configurations to have their inlets of a size and number to provide the required mass flow into the decelerator envelope consistent with the inflation interval of 1.5 sec. For the 120-deg conical AIRMAT cone having an auxiliary gas inflation source, gas pressure, gas volume, valve sizes, and valve numbers must also be compatible with the selected inflation interval.

Layout drawings of selected decelerator/vehicle combinations for the four decelerator configurations under study have been made or are in process. From these an assessment of the packaging, attachment, and deployment requirements or constraints can be gained. Additionally, realistic weight estimates for the ancillary equipment associated with these items can be made. It is indicated that packaged volume requirements are not beyond the range of practical considerations.

As previously indicated, dynamic stability characteristics of the selected configuration will be analyzed. In the case of attached BALLUTE configurations, a six-degree-of-freedom computer program is used. For the trailing BALLUTE, two additional degrees of freedom are included. The program has been debugged for use on the IBM 360 computer. Because of lack of data, linear variation of the aerodynamic coefficients with angle of attack will be assumed. Where experimental data are available, nonlinear variation of coefficients with Mach number will be utilized. Alternately, modified Newtonian theory or Sief's embedded flow theory will be relied upon to estimate values for aerodynamic coefficients.

Upon completion of this effort, the final comparison of the expandable decelerator characteristics will be made primarily in terms of engineering design considerations. In other words, since all the configurations have been "sized"

to accomplish essentially the same performance (attain specific target Mach number/altitude conditions), the relative advantages of one configuration compared with another will be associated with the following:

1. Decelerator system to total lander weight fraction
2. Effectiveness in attaining minimum oscillation amplitudes and rates
3. Complexity of attachments, stowage, deployment, and inflation requirements
4. Effect on terminal, stage-decelerator systems and operations
5. Effects on science payload and equipment

The last two items will be evaluated qualitatively under the scope of the present study. However, it is anticipated that valid and useful assessments can be made.

SECTION IV - RECOMMENDATIONS

As inferred by the statement of work for this program, a study of the present scope and application was not expected to yield data in sufficient detail for complete and final engineering designs of expandable decelerators for Mars atmosphere entry. Consequently, provision was made for making recommendations for areas requiring additional investigation and analyses. Additionally, descriptions of development, simulation, and proof-test procedures to qualify aerodynamic decelerator systems for the Mars Voyager lander mission, including the types of facilities required, are to be made.

The areas of additional investigation are indicated tentatively to include:

1. Detailed configuration design analyses associated with a specific entry vehicle and performance envelope, as broadly defined by the present study
2. Fabrication techniques and constraints for large-scale expandable structures of specified size and configuration
3. Wind-tunnel and ballistic range aerodynamic performance and stability tests of a specific configuration under simulated operating environments
4. Design and fabrication of a full- or near-full-scale, functional mockup (see Figure 15, for example) for packaging, deployment, and inflation tests in the NASA Ames or Langley full-scale wind tunnel facilities
5. Large-scale, free-flight simulation tests using rocket boost techniques such as those illustrated by Figure 16
6. Functional, environmental, and reliability tests of hardware

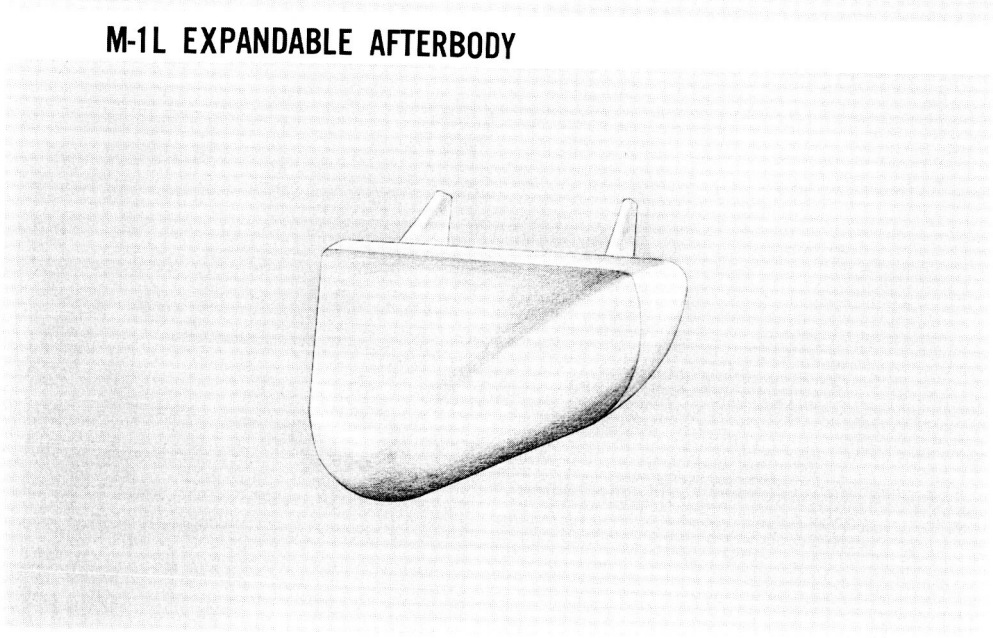

Figure 15

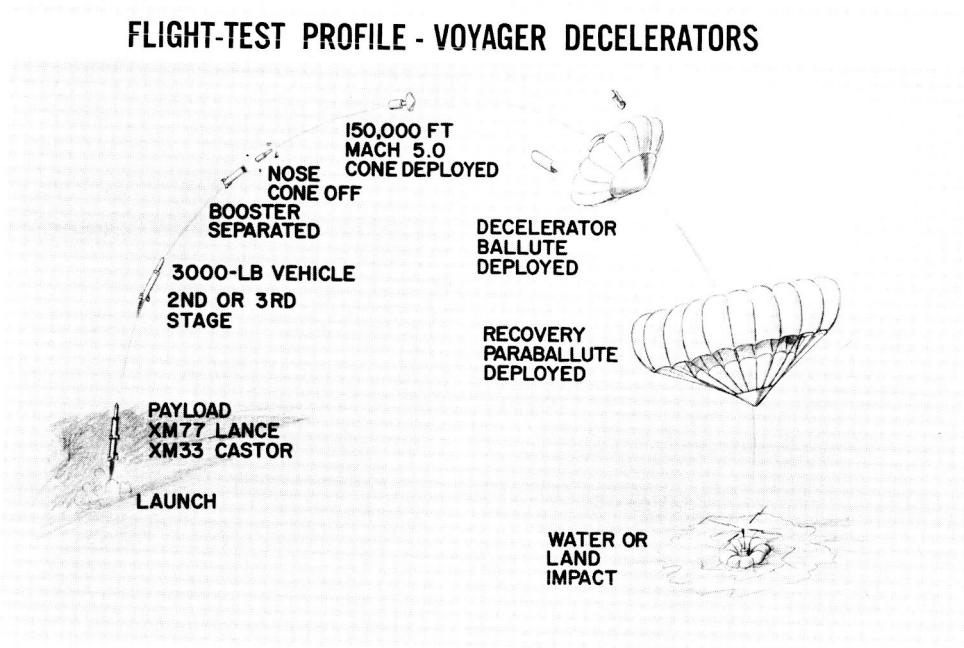

Figure 16

SECTION V - SUMMARY

In summary, Figure 17 indicates that the work accomplished to date under JPL Contract 951153 has resulted in the following information:

1. The analytical formulation of environmental factors and effects governing engineering applications, and the establishment of straightforward engineering techniques of analysis and design for expandable, terminal decelerators for Mars atmosphere entry.
2. The establishment of definitive trends toward minimum weight fractions for expandable decelerators with corresponding optimum values for initial operating Mach number to effect deceleration to a target

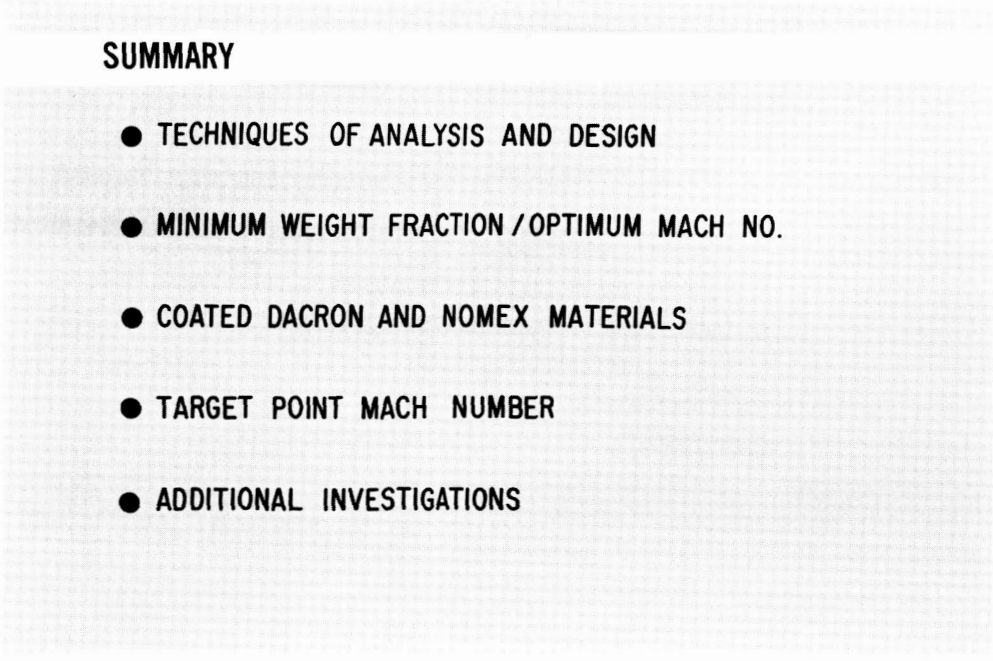

Figure 17

Mach number of 1.0 at altitudes of 10,000, 20,000, and 30,000 ft above the terrain for Mars entry vehicles having specific initial entry conditions.

3. The indication that Dacron material can be employed safely for fabrication of the decelerator devices under the combined aerodynamic and thermal loading environments encountered in Mars entry. For all cases analyzed at least minimum coatings must be employed to maintain acceptable porosity of the decelerator envelope. Under more severe heating conditions, additional coating thickness of practical proportions will be required to maintain the material temperature to acceptable design values.

4. The effect of varying target point Mach number from a nominal value of 1.0 has a measurable effect on decelerator size and altitude and, consequently, weight fraction.

5. Detailed engineering analysis, design, and simulation testing pointed toward specific configurations and performance envelopes within the broad range of values and trends defined by the present study will be required in future programs.

APPENDIX A - SUPPORTING DOCUMENTATION AND ANALYSES

The following material generated during work on JPL Contract No. 951153 has been used entirely to support the Interim Summary Report GER-12691 and is available only at the discretion of JPL.

1. Monthly Technical Letter Reports Nos. 1 through 7: JPL Contract No. 951153: December 1965 through June 1966.

2. Memoranda for file on Study of Expandable, Terminal Decelerators for Mars Atmosphere Entry: JPL Contract No. 951153.

   a. RSE-60302-3: Summary of contract work through March 1966. 2 March 1966.

   b. SM-9091: Structural and Weight Analysis, 28 April 1966.

   c. RSE-60426-29: Materials for Deployable, Inflatable Decelerators for the Mars Lander Capsule.

   d. RSE-60426-30: Sterilization Considerations Affecting Inflatable Decelerator Design for Mars Atmosphere Entry.

   e. RSE-60428-37: Free-Flight Test Simulation Technique.

   f. RSE-60505-10: Elements of Flow Analysis for the Mars Atmosphere Entry Decelerator.

   g. FD-735: Fabric Weight Requirements of the Mars Lander Decelerator System due to Aerodynamic Heating. 26 May 1966.

   h. FD-742: Additional Information on Fabric Weight Requirements due to Aerodynamic Heating. 7 June 1966.

APPENDIX B - SAMPLE TABULATION SCHEME FOR COMPARING CHARACTERISTICS OF DECELERATORS

Trajectory no. A4

Atmosphere VM7

Vehicle characteristics

Diameter, D_V (ft) 18.5

Mass (slugs) 94

Ballistic parameter, $\left(M/C_D A\right)_V$ 0.25

Drag area, $\left(C_D A\right)_V$ (sq ft) 376

Weight, W_E (Earth lb) 3025

Initial entry angle (deg) 25

Initial entry velocity (fps) 23,000

Target altitude (ft) 30,000

Target Mach no. 1.0

Decelerator configuration code

TB - trailing BALLUTE (80 deg with plain back)

AB - attached BALLUTE

TBB - tucked-back BALLUTE

AC - AIRMAT cone (120 deg)

Number	Characteristic	Dimension	Decelerator configuration			
			TB	AB	TBB	AC
1	Mach number at full-drag effectiveness	M = V/C	2.75	2	2.13	2.55
	Selection based on					
	Performance					
	Minimum weight trend		×	×	×	×
	Material limits					
2	Dynamic pressure at full-drag effectiveness	PSF	23	14.8	16	21
3	Altitude at full-drag effectiveness	Ft × 10^{-3}	46.8	39	40	45
4	Adiabatic wall temperature at full-drag effectiveness (turbulent flow)	F	440	250	300	340
5	Drag area at full-drag effectiveness, ($C_D A$)	Sq ft	316	842	800	694
6	Diameter	Ft	21.1	28.6	31.5	24.8
7	Drag coefficient, C_D (total)		0.903	1.308	1.025	1.433
8	Decelerator weight based on					
	Dacron material at 350 F	Lb	171	149.8	41.75	148.2
	Nomex material at 600 F	Lb	227	227	63	222.5
9	Minimum material unit weight for thermal environment based on					
	Dacron material at 350 F	Lb/sq ft	0.016	0.003	0.004	0.011
10	Total decelerator surface area	Sq ft	1958	3220	2000	678
11	Coating weight based on					
	0.01 lb/sq ft (min)	Lb	19.6	32.2	20	6.8
12	Total decelerator weight based on					
	Dacron material at 350 F	Lb	190.6	182	61.8	155
13	Main gas inflation source	Lb				10
	Ram air		×	×	×	
	Contained supply					×
14	Auxiliary gas inflation aid based on gas source					
	Alcohol/H_2O mixture at 0.013 lb/cu ft	Lb	69.9	163	93	
15	Packaging volume required (for the Dacron case) based on					
	Packing density = 20 lb/cu ft	Cu ft	9.54	9.1	3.09	7.75
	Packing density = 30 lb/cu ft	Cu ft	6.35	6.07	2.06	5.16
16	Inflated decelerator volume	Cu ft	5380	12520	7160	509
17	Estimated inflation time (from start of deployment)	Sec	1.5	1.5	1.5	1.5
18	Mach number at deployment initiation		2.92	2.11	2.24	2.7
19	Dynamic pressure at deployment	PSF	26.2	16	17.5	23.2
20	Adiabatic wall temperature at deployment	F	500	300	300	450
21	Centroid of inflated area	X_A/D_v				
22	Centroid of inflated volume	X_v/D_v	4.768	0.624	0.342	0.103
23	Moment of inertia of decelerator	Lb-ft-sec^2				
24	Moment of inertia of composite system	Lb-ft-sec^2				
25	Centroid of decelerator weight	X_o/D	4.789	0.728	0.446	0.103
26	Composite system cg position	X_{cg}/D_v				
27	Composite system cp position (M = 2.0 to 5.0)	X_{cp}/D_v				
28	Estimated C_{N_α} (average) = C_{Y_β} (M = 2.0 to 5.0)					
29	Estimated $\left(C_{m_q} + C_{m_\alpha}\right)$ (M = 2.0 to 5.0)					